

AXIAL TRANSPORT IN DRY BALL MILLS

Paul CLEARY

CSIRO Mathematics and Information Sciences, Clayton, Victoria 3169, AUSTRALIA

ABSTRACT

Ball mills are used for grinding of rocks, cement clinker and limestone from 10-100 mm feed sizes down to sub-millimetre product. They are typically rotating cylinders with diameters from 3-6 m and lengths from 6-12 m. The flow of particulate solids within these mills can be modelled using the Discrete Element Method (DEM). Typically, such modelling is done for short durations of a few mill revolutions and either in two dimensions or using thin three dimensional slices through the center of the mill with periodic boundary conditions in the axial direction. This facilitates an understanding of the radial motion of the charge, estimation of power draw and of liner wear, but it cannot provide information about axial transport within the mill. In this paper, we examine the axial transport in dry ball mills. This requires simulation of the entire mill and the full volume of the charge for significant periods of time (thousands of revolutions). We use a simple model for grate discharge that allows prediction of the time varying axial distribution of different particle sizes within a discharging ball mill. The distributions of sub-grate size 'fines' is shown to satisfy a one dimensional diffusion equation with the diffusion coefficient decreasing with grate size. A pulse test, where a single mass of fines is injected at the feed end, is able to quantify the residence time distribution of the fines.

INTRODUCTION

Simulation of tumbling and other types of mills by DEM offers the opportunity of better understanding the internal mill dynamics and of developing improvements to mill design and operation that can lead to large increases in mill efficiency and throughput. DEM has been used for modelling a wide range of industrial applications, particularly in milling. Early work on ball mills by Mishra and Rajamani (1992, 1994) has been followed by Cleary (1998b, 2001b). Similarly SAG mills were modelled by Rajamani and Mishra (1996) and subsequently by Cleary (2001a). Until fairly recently mill modelling was performed in two dimensions. Over the past five years this has been replaced by the simulation of thin axial slices with periodic boundary conditions (Cleary and Sawley, 2002 and Cleary, 2001c).

Detailed experimental validation has been performed for a centrifugal mill by Cleary and Hoyer (2000) and for a 600 mm diameter laboratory SAG mill by Cleary et al. (2003). These studies give reasonable confidence that the flow behaviour predicted accurately represent real particulate motions in dry mills.

In this paper we turn attention to the axial transportation of fine material in a ball mill that is able to discharge from one end. This requires simulation of the entire mill length.

DISCRETE ELEMENT METHOD

DEM is a particle-based technique. Each particle in the flow is tracked and all collisions between particles and between particles and boundaries are modelled. The contact force law used here is a linear spring-dashpot model where particles are allowed to overlap. The maximum overlap is fixed by the stiffness of the spring k , which provides a repulsive force. The dashpot contributes the dissipative component of the collision. The damping coefficient C , determines the effective coefficient of restitution for the material properties of the granular media. The spring and dashpot together define the normal force:

$$F_n = -k\Delta x + Cv_n \quad (1)$$

In the same way, the tangential force with a sliding friction limit is:

$$F_t = \min\left(\mu F_n, \int kv_t dt + Cv_t\right) \quad (2)$$

A general review of DEM and its variants can be found in Barker (1994). The algorithm for the simulation procedure developed and used at CSIRO Mathematical and Information Sciences is as follows:

- (1) A search grid regularly maintains a near-neighbour interaction list for all pairs of entities that might undergo collisions in that given period.
- (2) The near-neighbour list is used with the interaction model described above to identify and record all collisions involving particles and boundary particles. The forces on particle pairs and boundaries are evaluated.
- (3) All forces and torques are summed and used in the equations of motion for the particle system. These are integrated over a time suitable to resolve each collision.

This has been used to model various industrial granular flows. For details of the method and applications see Cleary, (1998a), Cleary and Sawley, (2002) and Cleary, (2003).

BALL MILL CONFIGURATION

The ball mill used in this study was 5 m in diameter and 7 m long. Figure 1 shows this ball mill with an opening cut in the front to allow the mill internals to be seen. The fill level was 30% by volume and the mill speed was 75% of the critical speed required to centrifuge particles. The charge consisted of rocks and balls, with balls making up 48.6% by volume of the charge. The ball size distribution used was 75 to 200 mm and the rock size distribution was 25 to 100 mm. The specific gravity of the rock was 4. The

total number of particles in this mill was 122,000 weighing 114 tonnes. The DEM simulations were performed in 3D. The simulations were of a dry mill, so there is no slurry motion to assist in the transport of the particulates, they move solely as a result of the particle dynamics. In these simulations we use a standard coefficient of restitution of 0.3 and a coefficient of friction of 0.75 (Cleary, 2001b).

It is important to note that 3D simulations, with these numbers of particles, over the timescales needed for significant axial transport to occur, take enormous amounts of computer time (of the order of many months).

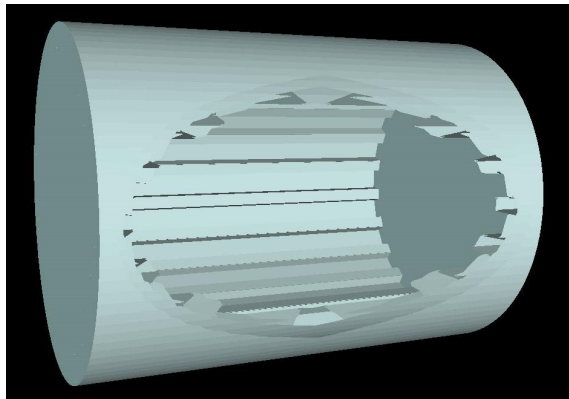


Figure 1: Ball mill used to study axial transport. The elliptical hole cut from the side allows the liner configuration to be viewed.

The simplest way to simulate a discharge grate in a flat ended mill is to make this permeable to particles below a certain grate opening size G . Such a grate is 100% efficient in that all fines that reach the grate immediately exit the mill. This is, of course, not the case for real mills, but it is a reasonable starting point for studying axial transport. This approach allows us to plausibly model the system and to study the critical physical processes in the axial direction.

END WALL EFFECTS

Most DEM models of mills involve taking a thin periodic slice from the middle of the mill. In this case we have included flat end walls, so it is useful to understand the effect of these walls on the flow of the particles. To begin, we simulate the flow in the mill with solid end walls. After a short time fairly strong axial segregation is observed near the end walls due to the high shear they induce. This concentrates finer material directly adjacent to the walls. Figure 2 shows the distribution of mass (dark grey curve in upper plot), particle number (light grey in the upper plot) and the average particle size (lower plot) in thin slices along the length of the mill (parallel to the end walls). We find that even when there is no inflow or outflow from the mill then composition gradients in the axial direction are still observed. The lower mass in the end regions means that the bulk density of the charge is much lower indicating that the end wall shear is inducing significant dilation to the charge. This enhances particle mobility and facilitates size segregation. This leads to the average size of particles near the end walls being around 15% smaller than in the bulk of the charge.

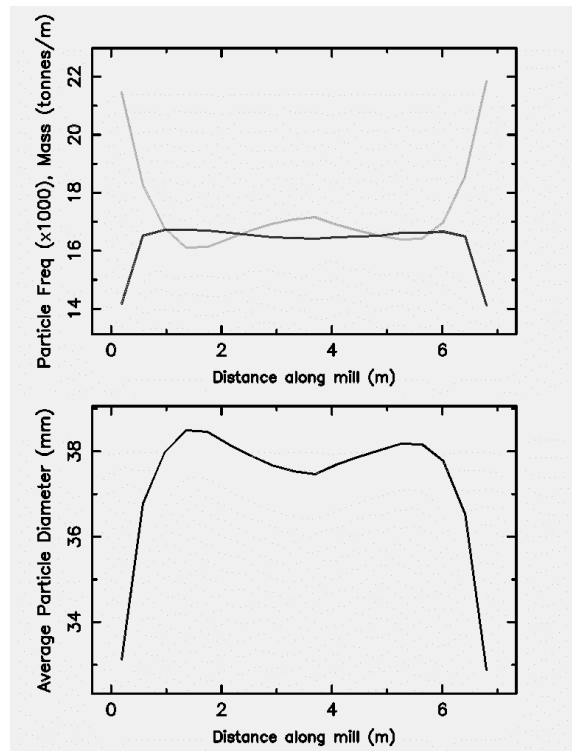


Figure 2: Distribution of mass and average particle size along the length of the mill after 4 minutes of operation.

AXIAL TRANSPORT AND MILL DISCHARGE

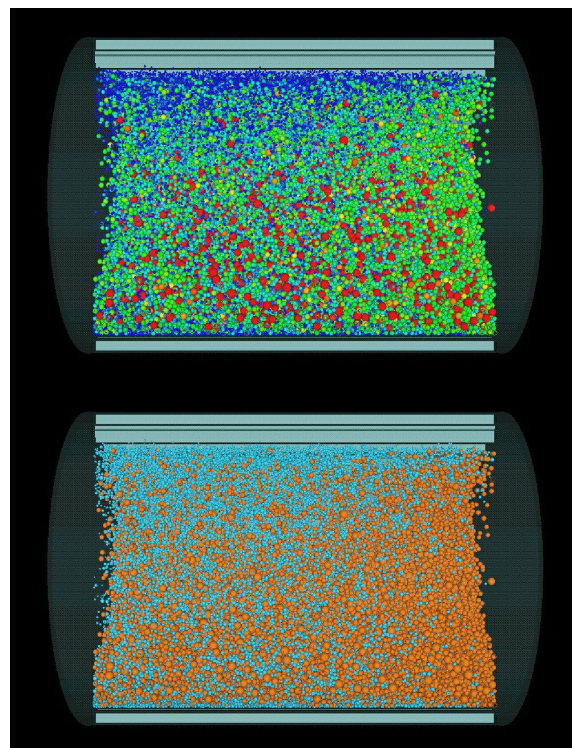


Figure 3: Visualisation of the charge after 4 minutes of operation. Particles are coloured by size in the top frame. In the bottom frame, coarse particles (larger than grate size G) are coloured orange and the smaller particles (fines) that are able to flow through the mill end are blue.

The ball mill is initially uniformly filled with rocks and balls which are perfectly mixed. Figure 3 shows the charge in the mill after 4 minutes of rotation (at 75% critical). The charge has been clipped by a vertical plane passing down through the center of the mill so that the internal distribution of particles can be seen. In the upper frame we see that there is very strong radial segregation leading to fines being concentrated near the liner at the top and bottom of the mill and a clear reduction in fines towards the discharge end of the mill. The lower frame shows that the majority of material near the discharge end is larger than the grate size (orange) indicating that significant discharge of fines (blue) has already occurred.

The change in the composition of the mill along its length can be evaluated by calculating the mass of coarse and fine fractions in vertical slices along the mill axis. The change in the distribution of these fractions allows us to follow the axial flow of fine material.

Figure 4 shows the time variation of this distribution of fines along the mill for $G = 60$ mm, a fill level of 30% and a mill speed of 75% critical. The black curve is the measured distribution from the DEM solution. The dashed line shows the initial distribution. At 10 s, around half the fine material in the end slice closest to the discharge end has flowed from the mill. The fines distribution is essentially constant along the rest of the mill.

After 1 minute of mill rotation, the fines level in the discharge end of the mill has dropped to about 1/3 of its original value. Fine material in the adjacent slices (up to 3 m from the discharge end) has now started flowing axially along the mill and is also discharging. There is an increase in the mass of fines in the first slice adjacent to the non-discharging end. This is caused by the segregation induced by the solid end wall shear (as reported in the previous section). This produces a slight reduction in fines around 1 m from the wall, which is the source of the additional fines segregating towards the solid end.

By 3 minutes, the amount of segregated fines near the solid end has reached its peak and the dip in the fines at around 1-2 m from the start of the mill is also reached its maximum. The fines fraction at the discharge end is now just 10% of its original level and the flow of fines from the middle of the mill towards the discharge end is observable back to the 2-3 m region.

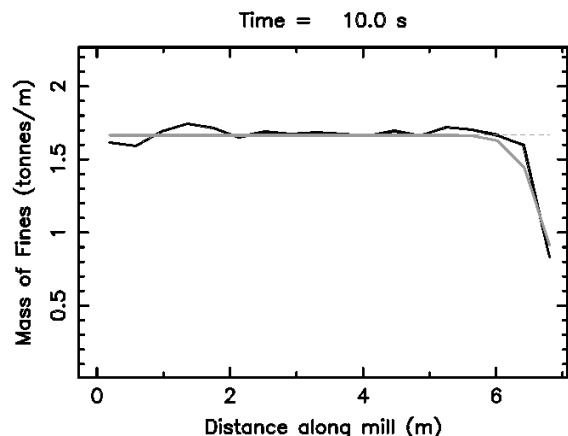


Figure 4: The mass of fines (per unit length) along the mill length is shown by the black curve. The grey curve is the best fit of an error function to the measured data.

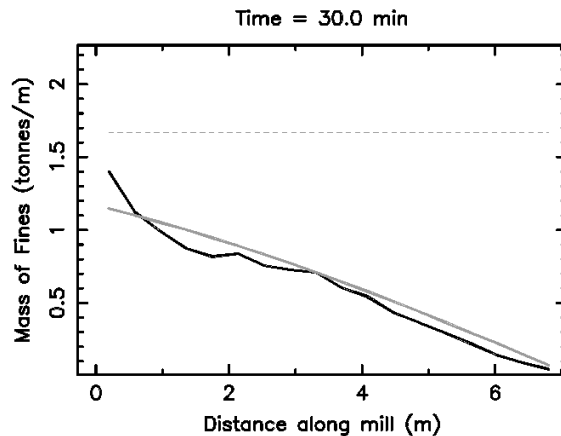
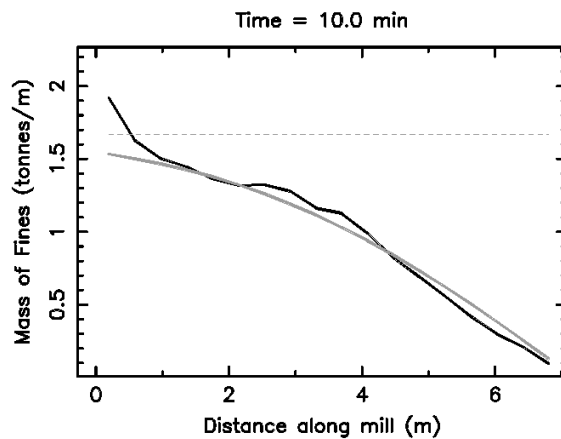
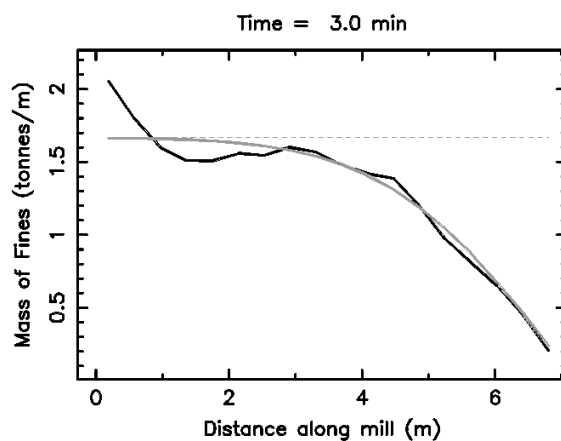
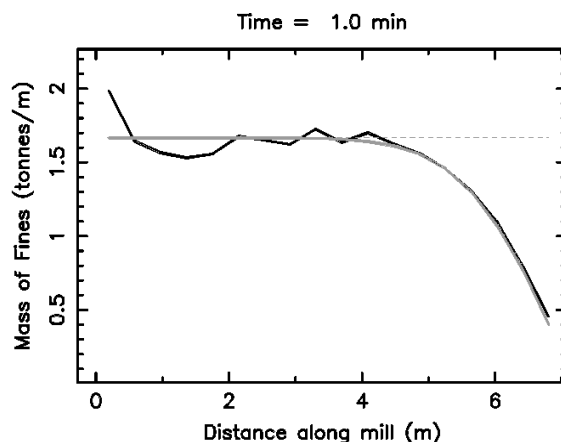


Figure 4 (ctd): The mass of fines (per unit length) along the mill length showing progressive reductions as mill discharge occurs for a grate size $G = 60$ mm.

At 10 minutes, a significant reduction in the amount of fines has occurred along the full length of the mill and even the fines enhanced region at the start of the mill is now losing fines.

By 30 minutes of operation, the fraction of fines at the start of the mill has been reduced by a 1/3 and there is very little fine material in the right half of the mill. This process continues until the fines are completely removed.

In the absence of slurry or fluids, a reasonable conjecture would be that this axial transport process for fines is a diffusive one. To test this a time varying error function is fitted to the DEM predictions of the axial distribution of the fines. The scaling coefficient in this solution is chosen by a least squares method to minimise the difference over both space and time of this solution from the DEM prediction. This solution is shown as the smooth grey curves in Figure 4. It is clear that this analytic solution fits the DEM predictions very closely. The only divergence is the segregation enhanced fines region and adjacent fines reduced region induced by the end wall shear at the start of the mill. An error function solution of this form is precisely the solution of a 1-D diffusion equation. This means that axial transport along a dry mill is purely diffusive and is not affected by the three dimensional details of the actual particle flows. The constant in the error function solution determined by the least squares process is then just a diffusion coefficient D . For this particular case $D = 0.0133$.

The diffusive nature of the dry axial transport can be understood when considering the nature of the particulate flow. Charge material is dragged upwards by the motion of the liner and then avalanches down the free surface or thrown through the air as a cataracting stream. The material in the cataracting stream is ballistic and its motion will be predominantly in the radial-circumferential plane of the mill (orthogonal to the mill axis). The cataracting material will therefore not generate any net axial transport of any of the components. In the avalanching stream, the material flow cascades from shoulder region. Consider the particulate flow from one particular axial location on that shoulder. As the material in that region avalanches down the surface, collisions with other particles cause the material undergo a random walk type of perturbation. Some particles are knocked in each axial direction with equal probability. This causes the material to spread out axially creating a widening fan shape as material moves down the free surface, with a particle having a normally distributed probability of being located at any specific axial location.

If this was a discrete avalanche this would lead to the fan shape of flow that is observed on point initiated avalanches on piles everywhere. If there is a composition variation along the mill, the half of the fan of spreading material that is on the discharge side is moving from a region of higher fines to one with lower fines. Material moving away from the discharge end is moving into a region of higher fines. If one considers the nature of the mass flow into and out of a slice of the mill's axial length, then some of the material is entering the slice from the discharge end and has a lower fines content, whilst material moving into the slice from the other end has a higher fines content. The distance from which the material has travelled (and therefore the magnitude of the enhanced or reduced fines level compared to that of the

slice) is determined by the width of the diverging avalanche which is in turn is governed by the random walk nature of the specific particle trajectories and the normal probability distribution in the axial direction for the spread of this material as it travels down the slope. This is a fundamental description of an inherently diffusive process. So in the slice considered there is a net transfer of finer material from upstream to downstream and the rate at which it is transported is controlled by the diffusive nature of the particles spreading out as they avalanche down the free surface of the charge. If one considers the overall material balance, there are equal amounts of material migrating into any specific slice, but the composition differences lead to a net migration of one of the components.

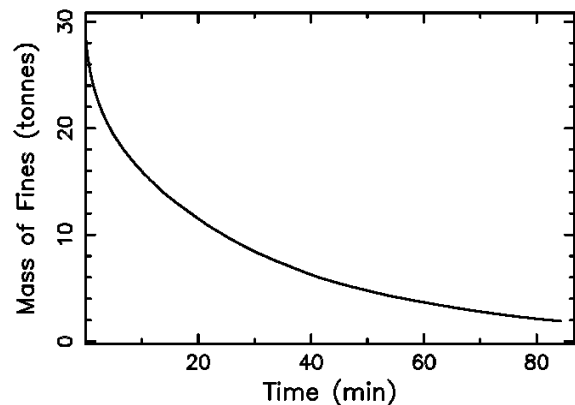


Figure 2: Mass of fines in the mill throughout the discharge process for a virtual grate size of 80 mm, a fill level of 30% and a speed of 75% critical.

Figure 2 shows the fines content of the mill over time. The amount of fines decreases sharply at the beginning when there are significant amounts of fines adjacent to the discharging end. As the process continues, the discharge rate decreases progressively. After 1.5 hrs of revolution, the fines content has been reduced from its initial level of around 28 tonnes to just 1 tonne. These very long time scales for full emptying of the mill make these DEM simulations substantial, since they involve 122,000 particles revolving for around 1500 mill revolutions (compared to typically 3 revolutions if one is studying the radial behaviour).

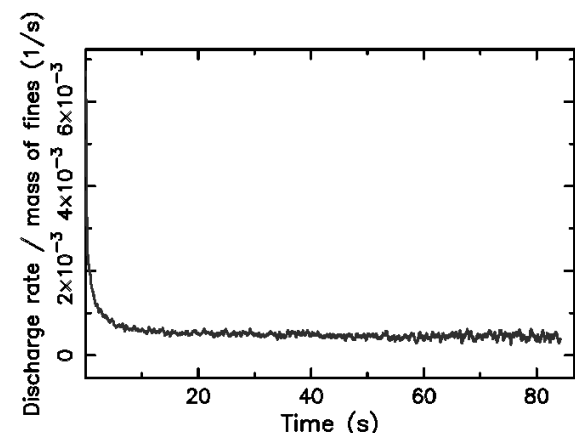


Figure 3: Ratio of the discharge rate to the amount of fines remaining in the mill throughout the discharge process for a virtual grate size of 80 mm, a fill level of 30% and a speed of 75% critical.

SIZE DEPENDENCE OF THE DIFFUSIVITY D

DEM simulations were performed with different discharge grate sizes in order to determine the sensitivity of the axial flow of fines to the size of the fine material. Table 1 shows the variation of the axial diffusion coefficient as a function of the fines particle size. This shows a weak but definite pattern of decreasing axial diffusivity with decreasing particle size. This can be understood by again considering the nature of the diverging fan of material flowing down the free surface from a single initiation point. The distance that a specific avalanching particle is able to travel axially depends on how much momentum it has and its chances of being trapped in the surrounding particle microstructure. As a particle gets smaller it is more able to fall into and become trapped in voids between larger particles and its decreasing momentum means it needs to collide less times before it ceases motion. These fundamental trends lead one to expect that material should become progressively more difficult to transport by pure diffusive processes as they become smaller. This is confirmed by the DEM simulation predictions. This behaviour is of course why dry mills are air swept to remove fines and why most mills are operated wet so as to wash the fines out of the mill significantly faster.

Maximum “fines” size	D
80 mm	0.0141
60 mm	0.0133
40 mm	0.0130

Table 1: Variation of axial diffusion coefficient with the size of the fines, for a fill level of 30% and speed of 75%.

Mills are operated with vastly varying fill levels according to local practices and current operating conditions, so it is useful to understand the effect that changing mill level has on axial fines transport. Table 2 shows the diffusion coefficients for three fill levels across a plausible operating range. We see that the axial diffusion increases when the fill level decreases from 30% to 20% and then decreases strongly with a further decrease to 10%.

There are two competing effects here, both essentially controlled by the length of the free surface, which in turn is determined by the fill level. At low fill, the length of the free surface is small and so therefore are the maximum widths of the diverging avalanches from the shoulder. As the fill level increases, so to does the dispersion in these longer avalanches. The axial diffusion is directly related to how far particles can spread axially in these diverging avalanches. The other effect comes from the turnover time, which is the time for material in the charge to circulate. For low fill levels, the smaller amount of charge turns over quickly, so material circulates more quickly and experiences many more avalanches. As the fill level increases the frequency with which a specific volume of material experiences avalanches leading to axial diffusion decreases. The combination of these effects means that for low fill levels, the avalanches are less effective, but there are many of them leading to a reasonable diffusion rate. As the fill increases, the surface length increases rapidly but the turnover time increases only moderately, so the

avalanches become much more effective but occur somewhat less frequently, leading to a moderately higher diffusion rate. As the fill level increases further, the length of the free surface decreases much less rapidly whilst the turnover time lengthens further. This means that the avalanches are becoming mildly more effective, but the rate of avalanches for a specific volume of charge decreases more rapidly leading to a decrease in the axial diffusion. For this mill and charge composition, the 20% fill level appears to have the balance of effects producing the highest overall axial transport rate.

Fill level	D
30%	0.0130
20%	0.0148
10%	0.0105

Table 2: Variation of axial diffusion coefficient with bed depth or fill level in the mill for a discharge size of 40 mm and a mill speed of 75% critical.

Mill speed is also an important factor in the operation of mills with higher speeds generally being pursued in order to increase mill throughput. Table 3 shows the predicted change in axial diffusion coefficient with mill speed across a representative range. The axial diffusion is strongest for the 70% of critical case and decreases almost linearly with increasing mill speed. This is easy to understand when considering that the axial diffusion results from the spreading of avalanches on the free surface and not from the cataracting stream of material. For a speed of 70%, the cataracting stream is fairly weak, but as the mill speed increases to 75% and then to 80%, the amount of cataracting material increases strongly and fairly steadily. The increasing importance of the cataracting along with the general increase in “turbulence” of the flow with increasing speed lead to the observed strong reduction in the effectiveness of axial diffusion.

Mill speed (% critical)	D
70%	0.0158
75%	0.0130
80%	0.0094

Table 3: Variation of axial diffusion coefficient with mill speed for a discharge size of 40 mm and fill level of 30%.

AN IMPULSE TEST

Figure 4 shows the axial movement of a pulse of fine material deposited into the mill at the feed end at the start of the simulation. The mill speed is 75% critical and the fill level is 30%. The fine material is just below 25 mm diameter and the grate size is $G = 25$ mm. Initially the material lands in a concentrated region around 2 m into the mill. This material diffuses in both directions. By 30 s, the peak is substantially smoothed and by 1 minute is just an inflection point. The fines first reached the discharge end after about 2 minutes. Thereafter, the fines distribution and the discharge behaviour are quite similar to the earlier experiments above.

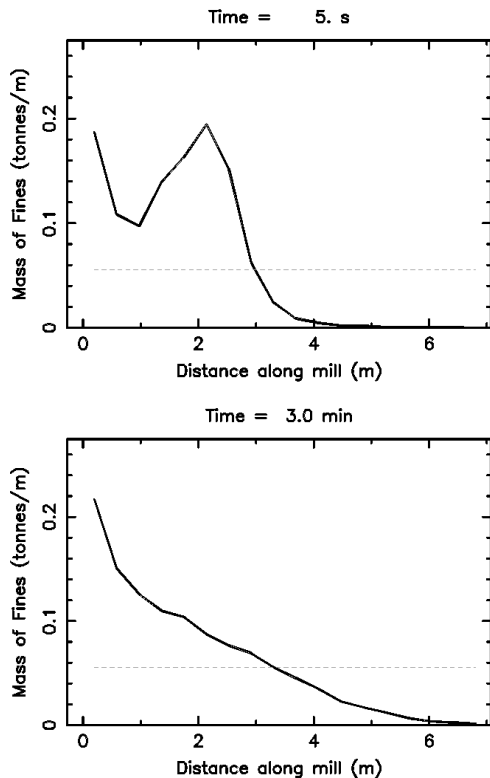


Figure 4: Pulse test showing the distribution of fines soon after they are dropped into the mill and after 3 minutes.

CONCLUSION

The dominant material flow in a mill is in the plane orthogonal to the axis of rotation. Charge material is dragged upwards by the motion of the liner and then either avalanches down the free surface or is thrown through the air as a cataracting stream. The material in the cataracting stream is ballistic and is thrown by the rotating mill in the radial-circumferential plane. This does not lead to any net axial transport. In the avalanching stream though, material spreads out via a random walk process resulting from particle collisions as it flows down the free surface. Avalanching material moving in the discharge direction enters regions with lower fines content, whilst material moving the other direction enters regions with higher fines content. In any specific slice of the mill there is therefore a net transfer of finer material from upstream to downstream and the rate at which it is transported is controlled by the diffusive nature of the particles spreading out as they avalanche down the free surface of the charge.

The diffusive nature of the axial transport in a dry mill is confirmed by monitoring the fines distribution in axial slices of the mill. The time and spatial variation of the fines predicted using DEM is very well represented by the solution of a 1-D diffusion equation. The discharge rate is found to be directly proportional to the mass of fines in the mill at any time, and so is initially high and decreases progressively as the mill empties.

The axial diffusion coefficient can be determined (from the 1-D diffusion solution) as a function of the operating conditions. Here we have found that it:

- Varies weakly with particle size with smaller particles being transported slightly more slowly.
- Decreases strongly with increasing mill speed due to the increasing fraction of cataracting material (which does not contribute to axial flow).
- At first increases and then decreases with increasing mill fill level due to the competing effects of increasing free surface length (which increases axial diffusion) and decreasing frequency of avalanching (which decreases the diffusion).

Simulation of axial transport processes in mills or rotating cylinders and the resulting axial variations in charge composition require very long computational times. Here we have been simulating a charge of 122,000 particles revolving for around 90 minutes or 1500 mill revolutions (compared to typically 3 revolutions if one is studying the radial behaviour) in order to observe the near emptying of fines from the mill.

REFERENCES

- BARKER, G.C. (1994), "Computer Simulations of Granular Materials", in: A. Mehta (Ed.), *Granular Matter: An Inter-Disciplinary Approach*, Springer, Berlin.
- CLEARY, P.W. (1998a), "Discrete Element Modelling of Industrial Granular Flow Applications", *TASK. Quarterly – Scientific Bulletin* **2**, 385–416.
- CLEARY, P. W., (1998b), Predicting charge motion, power draw, segregation, wear and particle breakage in ball mills using discrete element methods", *Minerals Engineering*, **11**, 1061-1080.
- CLEARY, P. W., (2001a), Modelling Comminution Devices using DEM, *Int. J. for Numer. Anal. Meth. Geomechan.* **25**, 83-105.
- CLEARY, P. W., (2001b), Charge behaviour and power consumption in ball mills: Sensitivity to mill operating conditions, liner geometry and charge composition, *Int. J. Min. Processing*, **63**, 79-114.
- CLEARY, P. W., (2001c), Recent advances in DEM modelling of tumbling mills, *Minerals Engineering*, **14**, 1295-1319.
- CLEARY, P.W. (2003), "Large scale industrial DEM modelling", to appear: *Engineering Computations*.
- CLEARY, P. W., AND HOYER, D., (2000), Centrifugal mill charge motion and power draw: comparison of DEM predictions with experiment, *Int. J. Min. Proc.*, **59**, 131-148.
- CLEARY, P.W., and SAWLEY, M. (2002), "DEM modelling of industrial granular flows: 3D case studies and the effect of particle shape on hopper discharge", *App. Math. Modelling*, **26**, 89–111.
- CLEARY, P. W., MORRISON, R., AND MORRELL, S., Comparison of DEM and experiment for a scale model SAG mill, *Int. J. Min. Processing*, **68**, 129-165, 2003.
- MISHRA, B. K., AND RAJAMANI, R. J., (1992), The discrete element method for the simulation of ball mills, *App. Math. Modelling*, **16**, 598-604.
- MISHRA, B. K., AND RAJAMANI, R. K., (1994), Simulation of charge motion in ball mills. Part 1: experimental verifications, *Int. J. Mineral Processing*, **40**, 171-186.
- RAJAMANI, R. K., AND MISHRA, B. K., (1996), Dynamics of ball and rock charge in sag mills, *Proc. SAG 1996*, Department of Mining and Mineral Process Engineering, University of British Columbia.